Power-law statistics and universal scaling in the absence of criticality

Jonathan Touboul[1,2,*] and Alain Destexhe[3,4]

[1]*The Mathematical Neuroscience Laboratory, CIRB/Collège de France (CNRS UMR 7241, INSERM U1050, UPMC ED 158, MEMOLIFE PSL), Paris, France*

[2]*MYCENAE Team, INRIA, Paris, France*

[3]*Unit for Neurosciences, Information and Complexity (UNIC), CNRS, Gif sur Yvette, France*

[4]*The European Institute for Theoretical Neuroscience (EITN), Paris, France*

(Received 29 February 2016; revised manuscript received 2 November 2016; published 31 January 2017)

Critical states are sometimes identified experimentally through power-law statistics or universal scaling functions. We show here that such features naturally emerge from networks in self-sustained irregular regimes away from criticality. In these regimes, statistical physics theory of large interacting systems predict a regime where the nodes have independent and identically distributed dynamics. We thus investigated the statistics of a system in which units are replaced by independent stochastic surrogates and found the same power-law statistics, indicating that these are not sufficient to establish criticality. We rather suggest that these are universal features of large-scale networks when considered macroscopically. These results put caution on the interpretation of scaling laws found in nature.

DOI: 10.1103/PhysRevE.95.012413

I. INTRODUCTION

Power-law statistics are ubiquitous in physics and life sciences. They are observed in a wide range of complex phenomena arising in natural systems, from sandpile avalanches to forest fires [1,2], earthquakes amplitude solar flares, website frequentation, as well as economics [3]. These distributions reveal unusual properties: The observed quantity has no typical scale and is not well characterized by its mean (when it exists). It is distributed over orders of magnitudes and large deviations are not exceptionally rare, in the sense that extreme events are far more likely than they would be, for instance, in a Gaussian distribution. These singular properties, combined with their ubiquity in nature, has attracted wide attention in applied science.

A number of theories were proposed in order to account for the presence of such power-law distributions. Some theories use an analogy with statistical physics systems and consider the presence of power-law scalings as the hallmark that the system could be operating at a phase transition. These theories associate a power law to a so-called notion of *criticality*: Classically, in statistical physics, *critical phenomena* are the behaviors occurring in systems in association with second-order phase transitions. These are largely thought to be universal although no proof has been provided yet. Indeed, a number of statistics are found in vastly distinct models and, in particular, in the Ising model [4] poised at its phase transition. The *critical* regime thus occurs only at very specific parameters values. At this regime, the properties of the system are particularly singular; in particular, a number of statistics are scale invariant, including, for instance, the size, duration, and shape of collective phenomena. The seminal work of Bak, Tang, and Wiesenfeld on the Abelian sandpile model [5] largely popularized the hypothesis that criticality may be the origin of power laws observed in nature. Indeed, despite the fact that parameters for criticality are very rare, systems may self-organize naturally at criticality (at the phase transition point) without requiring fine-tuning by a mechanism called self-organized criticality (SOC) [1]. This remarkable theory has sometimes led to the conclusion that natural systems were critical, based on the identification of power-law relationships in empirical data (see Refs. [2,5] for reviews).

While power laws, as well as phase transitions (thus criticality), are well identified in models, a number of authors have underlined the importance of being cautious when claiming power-law behavior in finite systems, questioning their relevance or usefulness [6,7]. In particular, Stumpf and Porter [6] aptly noted the importance of taking a nuanced approach between theoretical and empirical statistical support reporting a power law, as theories arise from infinite systems while real systems and usual data sets are finite.

In physics, several alternative theories have been proposed to account for the presence of power laws (see, e.g., Ref. [3] for a review). In particular, it was noticed very early that a pure random typewriter (a monkey sitting at a typewriter) would generate texts with a power-law distribution of word frequencies [8] identical as the one observed in data. This work brilliantly showed that a power law may arise from purely stochastic mechanisms, evidencing that some power-law distributions may not reflect deep structures in the data. Li [9] formalized Miller's theory, highlighting the fact that combinations of exponentials naturally yield power-law relationships. Bouchaud and others [10,11] noted that the inverse of regularly distributed quantities may show power-law distributions. Newman and colleagues showed that random walks generate several statistics scaling as power laws [3]; Yule introduced a process with broad applications, particularly in evolution, naturally associated to power-law distributions; and Takayasu and collaborators [12–14] showed that systems with aggregation and injection naturally generate clusters of size scaling as a power law with exponent $-3/2$. In neuroscience, Benayoun, Wallace, and Cowan have shown that neuronal networks models in a regime of balance of excitation and inhibition also provide power-law scalings of avalanches [15]. All of these mechanisms are independent of any phase

*jonathan.touboul@college-de-france.fr

transition and arise away from criticality from a particular way of considering a random process.

The hypothesis that networks of the brain operate at criticality was introduced a decade ago with the development of recording techniques of local populations of cells and the analysis of specific events corresponding to collective bursts of activity separated by periods of silence. The first empirical evidence that neuronal avalanches may show power-law distributions of duration or size was derived from the analysis of neuronal cultures *in vitro* activity [16]. Based on an analogy with the sandpile model, these bursts were seen as "neuronal avalanches" and were apparently distributed as a power law with a slope close to $-3/2$, consistent with the distribution of sandpile avalanches. These *in vitro* findings were based on indirect evidence of spiking derived from local field potentials and extracellular signals associated with the summation of postsynaptic potentials [bursts produce negative peaks in the local field potential (LFP) signals] and affected by a number of events unrelated with spiking activity. Similar LFP statistics were later found *in vivo* in the awake monkey [17] and in the anesthetized rat [18]. These empirical evidences were used to draw strong conclusions on neural coding: The presence such power laws would ensure maximized information capacity, dynamic range, and information transmission [19,20]. However, the method of analyzing the amplitude of negative LFP peaks was shown to produce spurious power-law scaling [21] regardless of the spike activity of cells. Indeed, identical scalings were found in surrogate data (positive LFP peaks that are independent of spiking activity), and also arise in elementary purely stochastic signals, such as excursions of Ornstein-Uhlenbeck processes through thresholds away from the mean or in one-dimensional random walks [22,23]: Both duration and time of excursions show power-law statistics and display shape invariance. It was further shown in that both in data and surrogate models, statistical significance of these power laws of LFP peak was poor and depended on the threshold chosen. In Ref. [24], Dehghani and collaborators have made a statistical analysis combining multielectrode *in vivo* recordings from the cerebral cortex of cat, monkey, and human and did not confirm the presence of power laws. The data rather showed an optimal fit with two independent exponential processes.

The poor statistical significance of LFP avalanche analysis and the ambiguous results it yields has motivated an in-depth exploration of *in vitro* spiking data of cultures of neurons [25]. In this remarkable work, the authors used multiunit data from *in vitro* cultures and addressed a number of properties of critical systems reported by Sethna *et al* unified theory of criticality of statistical systems [26]. Of crucial importance in this theory are power-law scalings of specific events and the relationship between the different scaling exponents. Friedman and collaborators [25] revealed that the data was consistent with Sethna *et al.* theory, since power-law scalings of both avalanche size and duration were reported, with slopes consistent with the critical exponents of $-3/2$ and -2, respectively, but also the existence of a universal mean temporal profiles of firing events collapsing under specific scaling onto a single universal scaling function, thereby providing a more substantial analogy between this *in vitro* system with statistical physics models at criticality.

In the present paper, we show that these observations can arise naturally in neuronal systems that are not at criticality. We also provide a theoretical explanation for this, as well as analytic access to some of the relevant properties of such systems.

II. AVALANCHES IN SPIKING NETWORK MODELS

We start by investigating the avalanche distributions generated by the classical model of a spiking neuronal network with excitatory and inhibitory connections introduced by Nicolas Brunel in Ref. [27]. This model describes the interaction of n neurons described through their voltage $(v_i)_{i=1\cdots n}$ that decays to reversal potential in the absence of input, receives external input and spikes from interconnected cells, and fires action potentials when the voltage exceeds a threshold θ. In detail, the voltage of neuron i satisfies the equation:

$$\tau \frac{dv_i}{dt} = -v_i + R\tau \sum_{j=1}^{n} J_{ij} \sum_{k\geqslant 0} \delta\big(t - t_j^k - D\big), \qquad (1)$$

while $v_i \leqslant \theta$ and where τ denotes the time constant of the membrane and R its resistivity. The input received by the neuron are Dirac δs. Neuron i receives the kth impulse of neuron j, emitted at time t_j^k, after a delay denoted D and assumed constant, which alters its membrane potential of a quantity proportional to J_{ij}. Brunel's model assumes that these coefficients are zero except for a fixed number of cells randomly chosen in the excitatory and inhibitory populations, for which the coefficient J_{ij} have fixed values J and $-gJ$, respectively (see Ref. [27] for details). This model is particularly interesting for its versatility and ability and to produce diverse spiking patterns. One can classify the regimes of activity in terms of levels of synchrony and regularity, and different regimes emerge as a function of the relative levels of excitation and inhibition and the input, which can be identified through the computation of precise bifurcation curves [27]. The thus-obtained regimes are termed *activity states* to distinguish these from the statistical mechanics notion of *phase*: The regimes are here separated by bifurcations occurring in the mean-field limit of the system. Of special interest are the *asynchronous irregular* (AI) states, in which neurons fire in a Poisson-like manner, with no period of silence (and hence no avalanche). This activity is evocative of the spike trains observed experimentally in awake animals. Such sparsely connected networks can also display periods of collective activity of broadly distributed duration interspersed by periods of silence, called *synchronous irregular* (SI) regimes, known to reproduce the qualitative features of spiking in anesthetized animals or neuronal cultures. Although partially ordered and partially disordered, SI regimes occur for a wide range of parameter values (all in inhibition-dominated regimes) [27] and are not very sensitive to modifications of biophysical parameters. The SI regime is not at a transition in the activity regime; within this region, chaotic activity takes place. Indeed, inhibition dominates the excitation, thus when the activity spreads throughout the network, it triggers massive inhibition that naturally silences the network. This is what we observe in simulations of the Brunel model (Fig. 1) [28]. We investigate the statistics of spike units in both cases (see Fig. 1).

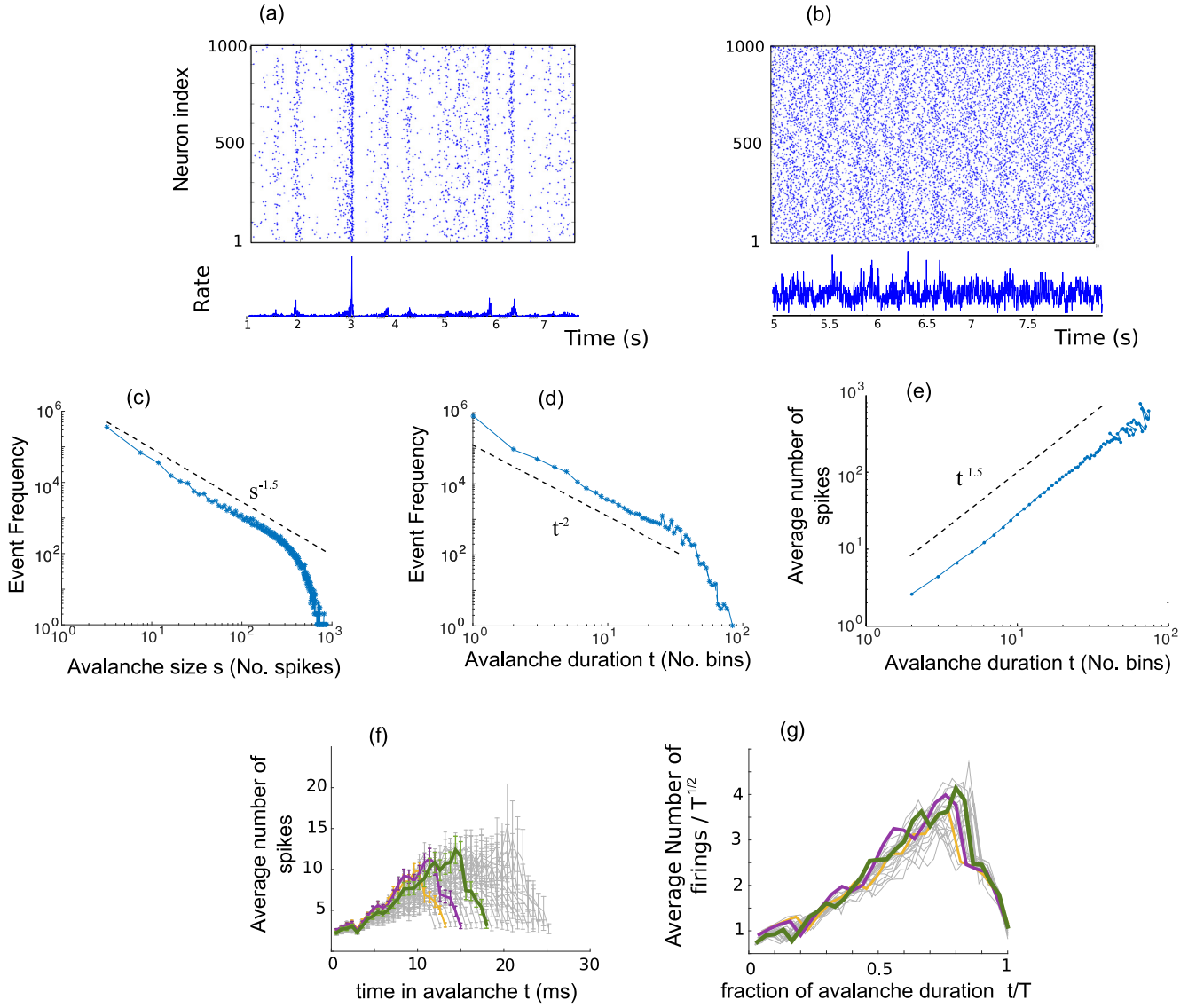

FIG. 1. Avalanche spike statistics in the sparsely connected networks [27] with $N = 5000$ neurons in the SI and AI states. (a) Raster plot of the SI together with the firing rate (below). (b) Raster plot in the AI state: Spiking is asynchronous and faster (notice that the time window is shorter compared to A for legibility); no silence period arises. Parameters as in Ref. [27], Fig. 2(d)] with $g = 4$ (excitation-dominated regime) and $\nu_{\rm ext}/\nu_{\rm thresh} = 1.1$. In the SI states (c), avalanche size (number of spikes) and (d) avalanche duration (number of bins) scale as power law (dashed line is the maximum likelihood fit), and averaged avalanche size scales as a power law with the duration avalanche duration according to the universal scaling law [26] (e). Average avalanche shapes collapse onto the same curve [(f) and (g)] very accurately. Avalanche shapes from 20 to 40 bins are plotted in gray, and three of the same size as in Ref. [25] are colored and with distinct thicknesses. Parameters as in Ref. [27], Fig. 2(d)] with $N = 1000$, $g = 5$ (inhibition-dominated regime), and $\nu_{\rm ext}/\nu_{\rm thresh} = 0.9$.

First, in the AI state, the sustained and irregular firing does not leave room for repeated periods of quiescence at this network scale, preventing the definition of avalanches [see the raster plot in Fig. 1(b)] [29]. This sharply contrasts with the SI state, in which we can define avalanches which display the same statistics assumed to reveal criticality in cultures [25]. Figure 1(a) represents the raster plot with typical avalanches taking place. Strikingly, both avalanche duration and avalanche size show excellent fit to a power law, validated by Kolmogorov Smirnov test of maximum likelihood estimator [30], and the exponents found are consistent with those found in neuronal cultures [25]. In particular, we find that the size s of the avalanches (number of firings during one avalanche) apparently scales as $s^{-\tau}$ with $\tau = 1.42$ [Fig. 1(c)], close to the theoretical value of 3/2 (plotted on the figure for indication) and to the neuronal culture scaling (1.7 reported in Ref. [25]). Using the Kolmogorov-Smirnov test [30], we have tested the hypothesis that the data are distributed as a power law and validated the hypothesis (Kolmogov-Smirnov distance 0.0097, p-value $p > 0.99$). This is also the case of the distribution of the duration t of the avalanches, found scaling as $t^{-\alpha}$ with $\alpha = 2.11$ [Fig. 1(d)], close to the theoretical value of 2 for critical systems and from the experimental value of 1.9 found in neuronal cultures [25]. The Kolmogorov-Smirnov distance with a pure power law is very low, evaluated at 0.031, which leads to a high p-value $p = 0.99$, validating clearly the

hypothesis of a power-law distribution of avalanche durations. Similarly to what was observed experimentally, the fit is valid on two octaves and drops down beyond [31]. This exponential drop is classically related to subsampling effects. We validated the presence of finite-size cutoffs by varying the size of the system and found indeed that as the network size increases, the fit with a power-law distribution is valid on larger time intervals and the cutoff only arises at later times (see Fig. 6). Also consistent with neuronal data and crackling noise, we found that the average avalanche size scales very clearly as a power of its duration, but with a positive exponent $\gamma = 1.50$, not consistent with the crackling noise relationship between exponents

$$\gamma = \frac{\alpha - 1}{\tau - 1} \tag{2}$$

that predicts an exponent equal to $\gamma = 2.64$ but, however, is quantitatively consistent with the *in vitro* data of Ref. [25]. We have also investigated the shape of the avalanches of different durations. We have found that, similarly to critical systems or to *in vitro* data, the avalanche shapes collapsed onto a universal scaling function [Fig. 1(e)] when time is rescaled to a unit interval and shape rescaled by $T^{\gamma-1}$ where $\gamma = 1.5$ is the power-law exponent of the average size.

These scalings are not specific to the particular choice of parameters used in our simulations: We consistently find, in the whole range of parameter values corresponding to the SI state of Brunel's model, and in particular, away from any transitions, similar apparent power-law scalings with similar scaling exponents (see Fig. 7). Moreover, we confirmed, in addition to the fact that this regime is away from all transitions between the different network activity, that the system is not at criticality by showing that relaxation towards the SI regime after perturbation is fast (within milliseconds) within the region considered, although it does slow down close to the transition point (see Fig. 8). We conclude that these statistics are valid in a whole regime of the system where the activity is synchronous irregular, and neither at a transition of the model nor in a regime consistent with the slow decay of perturbations associated to critical regimes. Therefore, finding power-law statistics in neuronal avalanches with exponents 1.5 and 2 does not reveal that the system operates at criticality but rather seems a property of synchronous irregular states.

The SI states are prominent in neuronal activity, especially in anesthesia and neuronal cultures. It is precisely in these situations that power-law distributions of spike avalanches were reported experimentally [16,18]. This regime differs from the awake activity where neurons fire in an AI manner. In these regimes, power laws and criticality were reported based on LFP recordings [17]. We will come back to experimental evidences of power laws in local-field potentials recordings of the activity in Sec. V.

III. AVALANCHES AND BOLTZMANN MOLECULAR CHAOS PROPERTY

The observation of such scaling relationship in simple models of neuronal networks away from criticality and for a broad range of parameter values suggests that the observed scaling is related to properties of the systems that are independent of the notion of criticality and that may be relatively general. These may therefore be related to the properties of the network activity that we now describe in more detail.

A. Propagation of chaos in neural networks models

The classical theory of the thermodynamics of interacting particle systems states that in large networks (such as those of the brain), the correlations between neurons vanishes. This is also known as the Boltzmann molecular chaos hypothesis (*Stoßzahlansatz*) in reference to the hypothesis that the speed of distinct particles should be independent, key to the kinetic theory of gases of Ludwig Boltzmann [32]. In mathematics, this property is called *propagation of chaos* and is rigorously defined as follows:

Definition 1. For $(X_1^n, \ldots, X_n^n)$ a sequence of measures on $(\mathbb{R}^d)^n$. The sequence is said X chaotic if for any $k \in \mathbb{N}$ and $i_1, \ldots, i_k$ a set of indexes independent of n we have $(X_{i_1}^n, \ldots, X_{i_k}^n)$ converge to k independent copies of X as $n \to \infty$.

In our context, in the limit of large networks, neurons behave as independent jump processes with a common rate, which is the solution of an implicit equation. This property is at the core of theoretical approaches to understand the dynamics of large-scale networks [27,33–35]. In the case of Brunel's model, it is shown that since two neurons share a vanishing proportion of common input in the thermodynamic limit, allowing us to conclude that the correlation of the fluctuating parts of the synaptic input of different neurons are negligible. This leads the author to conclude that the spike trains of different neurons are independent point processes with an identical instantaneous firing rate $\nu(t)$ that is the solution of a self-consistent equation (see Ref. [[27], p. 186, first column]). In that view, except in the case of constant firing rate (the asynchronous irregular state), neurons always show a certain degree of synchrony due to the correlations of the instantaneous firing rates of different neurons.

Mathematically, several methods were developed for interacting particle systems and gases (see, e.g., Ref. [36] for an excellent review). It is shown that, generically, systems of interacting agents, with sufficient regularity, show propagation of chaos. All these results are in particular valid for neuronal networks, as was shown recently in a number of distinct situations. Large-n limits and propagation of chaos was demonstrated for large networks of integrate-and-fire neurons [37], firing-rate models with multiple populations [38], and conductance-based models even in the large time regime [39] and was shown to hold in realistic network models incorporating delays and the spatial extension of the system [40,41]. Rigorous methods of convergence of particle systems show that the *empirical measure* of the system:

$$\hat{\mu}_n = \frac{1}{n} \sum_{j=1}^{n} \delta_{x_i}$$

converges in law towards a unique solution. A very powerful and universal mathematical result demonstrated in Ref. [[42], Lemma 3.1] ensures that that the convergence of the empirical measure of a particle systems towards a unique measure implies propagation of chaos. Several methods may be used

to show convergence of the empirical measure, including in the case of neuroscience, coupling methods [41], compacity estimates [37], or large deviations [43].

These results indicate that a universal form of activity emerges from neural networks, whereby neurons are independent copies of the same process. Before investigating the avalanche statistics of such regimes of activity, let us discuss the plausibility of the existence of these regimes in neuronal data.

B. Decorrelation in experimental data and models

In natural environments, regularity of sensory input to the brain may create strong and long-range correlations in space and time [44–47]. It soon appeared that these correlations would be detrimental for the brain to encode sensory stimuli and detect changes efficiently [48,49]. Theoretical models of the visual system in particular have shown that decrease of redundancy by decorrelation was important for efficient encoding of natural images [50–52]. Such a decrease was confirmed experimentally. In Ref. [53], the authors used high-density two-dimensional electrode array and found in particular a marked exponential decay of correlation of excitatory cells. A clear confirmation of decorrelation even for closeby cells receiving similar input was recently brought in a remarkable experimental work where chronically implanted multielectrode arrays were developed and implanted in the visual cortex of the macaque [54]. This protocol produced exquisite data allowing us to show that even nearby neurons, generally thought to be strongly connected and to receive a substantial part of common input showed a very low level of correlation. Similar decorrelation results were reported in the rodent neocortex [55] with the same level of accuracy.

The origin of this decorrelation is still controversial and several assumptions were formulated, including the role played by adaptation ionic currents that could play central role in temporal decorrelation [56], negative correlations associated with the coevolution of excitatory and inhibitory cells activity [55], or sophisticated and robust mechanisms relying on neuronal nonlinearities and amplified by recurrent connectivities [57], that was compatible with pattern decorrelation observed in the olfactory bulb of the zebra fish.

All these experimental findings confirm that regimes in which neurons are independent are plausible representations of neural networks activity. We now investigate the avalanche statistics of such networks.

C. Statistics of networks in the molecular chaos regime

Both the mathematical analysis of neuronal network models and fine analysis of the structure of spike trains motivates the study of ensembles of neurons that are independent but with common nonstationary statistics. The simplest model one could think of is to consider a collection of independent Poisson processes with identical time-dependent rates.

In that view, cells with constant firing rates resemble AI regimes. To generate a stochastic surrogate of the SI regime, the common rate of the cells should display nonperiodically periods of silence. An obvious choice would be to replay the rates extracted from the SI state, and indeed such a surrogate generated power-law statistics (not shown), but in this case we could not rule out whether the power-law statistics are encoded in the rate functions. To show that this is not the case, we generated a surrogate independent of the rate functions by using a common rate of firing of the neurons given by the positive part ρ_t^+ of the Ornstein-Uhlenbeck process:

$$\dot{\rho}_t = -\alpha\rho_t + \sigma\xi_t$$

with (ξ_t) a Gaussian white noise. This choice is interesting in that although periods of silence do not occur periodically, the duration between two such silences have a finite mean. Actually, the distribution of excursions shape and duration of the Ornstein-Uhlenbeck process are known in closed form [58]. These distributions are, of course, not heavy tailed: They have exponential tails with exponent α which is the time scale of decay of the process.

We investigated the collective statistics of $N = 2000$ independent realizations of Poisson processes with this rate. The resulting raster plot is displayed in Fig. 2(a). While the firing is an inhomogeneous Poisson process, macroscopic statistics show power-law distributions for the size [$\tau = 1.47$, Fig. 2(b)] and for the duration [$\alpha = 1.9$, Fig. 2(c)], both statistically significant [30] and consistent with critical exponents. Again, a linear linear relationship between average avalanche size and duration is found, with a coefficient evaluated to $\gamma = 1.4$ and explaining all the variance but 6×10^{-4}. Again, this coefficient is not consistent with the crackling relationship (2). Notwithstanding, we found that the averaged shape of avalanches of a given duration collapse onto one universal curve when the amplitude is rescaled by the duration to the power $\gamma - 1$ [Figs. 2(d) and 2(e)].

Of course, these statistics are not related to the nature of the rate chosen. We display in Fig. 9, for instance, the avalanche statistics of independent Poisson processes with a rate given by the positive part of a reflected Brownian, and we find exactly the same power-law statistics of avalanche shapes and durations, as well as a very nice collapse of avalanche shapes.

D. Analytical derivations in the stationary and slow rate regime

In this simple model, it is actually very simple to indeed compute explicitly the distribution of avalanche duration, for instance. Disregarding the Poisson nature of the firings and the type of rate chosen, we can indeed write down the probability for an avalanche of duration t to occur at a specific time. These distributions can be computed analytically in cases where the spiking is described by a point process. In that case, denoting by $p(t)$ the probability for a neuron to spike in the time interval $[t, t+\delta]$, the probability to observe an avalanche of size τ starting at time t^* in a collection of n independent realizations is

$$q(t^*)^n q(t^*+\tau+1)^n \prod_{t=1}^{\tau}[1-q(t^*+t)^n],$$

where $q(t) = q_t := 1 - p(t)$. Assuming stationarity, the probability of finding an avalanche of duration τ is given by

$$\int_{[0,1]^{\tau+2}} q_0^n q_{\tau+1}^n \prod_{t=1}^{\tau}\left(1-q_t^n\right) d\rho_{\tau+2}(q_0,\ldots,q_{\tau+1}),$$

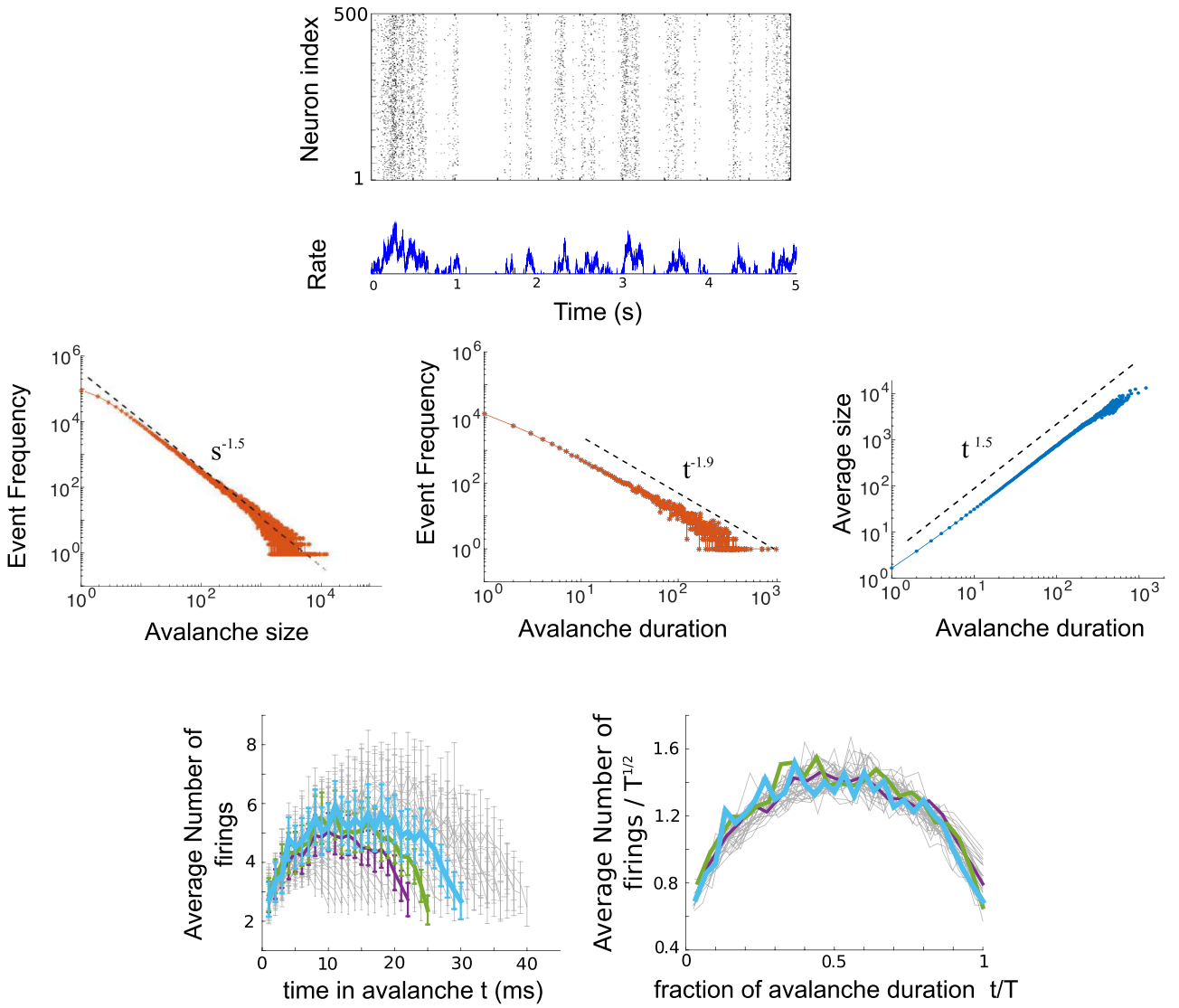

FIG. 2. Avalanches statistics in the independent Poisson model with Ornstein-Uhlenbeck firing rate ($\alpha = \sigma = 1$). Apparent power-law scalings, together with scale invariance of avalanches shapes. Avalanches of size 10 to 40 in gray, and three specific trajectories highlighted.

where ρ denotes the joint probability for the firing rate to have a specific sequence of values $(q_0, \cdots, q_{\tau+1})$.

This formula remains quite complex. Assuming now that the rate is extremely slow compared to the avalanches, one can simplify further the probability of p_τ^0 of an avalanche of size τ:

$$p_\tau^0 = \int_0^1 q^{2n}(1-q^n)^\tau \rho_1(q)dq,$$

and thus with a simple change of variable:

$$p_\tau^0 = \frac{1}{n}\int_0^1 x^{1+\frac{1}{n}}(1-x)^\tau \rho_1\left(x^{\frac{1}{n}}\right)dx.$$

As expected, when $n \to \infty$, the probability of having an avalanche of prescribed, finite duration goes to zero as $1/n$. The typical shape of the distribution can be obtained by rescaling this probability by n. Since we are interested in the logarithmic shape of the distribution, we disregard any multiplicative constant. As $n \to \infty$, we thus obtain that the probability profile converges towards a universal limit independent of the particular shape of the distribution ρ, precisely given by:

$$p_\tau^{0,\infty} \propto \int_0^1 x(1-x)^\tau dx = \frac{1}{(\tau+1)(\tau+2)},$$

which is indeed a power law with exponent -2, identical to the one arising in critical systems, consistent with those reported in neuronal data [25], in neuron models (Fig. 1), and in surrogate systems (Fig. 2).

We now show that this extends to the distribution of avalanche size and the scaling of the mean avalanche size with duration. Indeed, the size of avalanches of duration τ have a binomial distribution, corresponding to $s-\tau$ successes among $(n-1)\tau$ independent Bernoulli variables with probability of success $1-q(t)$. Moreover, the De Moivre-Laplace theorem [59] ensures convergence as n increases towards a normal variable with mean $(n-1)\tau p(t)$ and variance $(n-1)\tau p(t)q(t)$. Using again our separation of time scale and stationarity

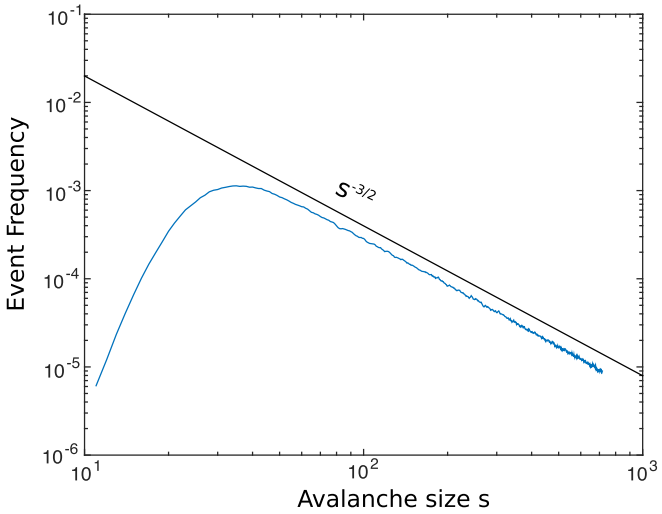

FIG. 3. Universal shape of the avalanche size distribution in the slow rate and large-n limit.

hypotheses, we find the probability the probability of finding an avalanche of size s and duration τ averaged on the firing rate:

$$\bar{p}^n(s,\tau) \sim \int_0^1 e^{-\frac{[s-\tau-n(1-q)\tau]^2}{2nq\tau(1-q)}} \frac{q^{2n}(1-q^n)^\tau}{\sqrt{2\pi nq\tau(1-q)}}\rho(q)dq,$$

which converges, as $n \to \infty$, towards:

$$\bar{p}^\infty(s,\tau) \sim \int_0^1 e^{\frac{[s-\tau[1+\log(u)]]^2}{2\tau\log(u)}} \frac{u(1-u)^\tau}{\sqrt{2\pi\tau\log(u)}}\,du.$$

We thus obtain at leading order the size distribution:

$$\mathcal{P}(s) \sim e^s \sum_{\tau=1}^{s} \int_0^1 e^{\frac{(s-\tau)^2}{2\tau\log(u)}} \frac{u[\sqrt{u}(1-u)]^\tau}{\sqrt{2\pi\tau\log(u)}}\,dx. \qquad (3)$$

It is hard to further simplify this formula, but it can be easily evaluated numerically. We depict the result of this computation in Fig. 3 and illustrate the apparent power-law scaling with slope $-3/2$.

Eventually, we obtain for the average size A_τ of avalanches of duration τ:

$$A_\tau \sim \int_0^1 \int_{s=\tau}^{\infty} s\, e^{\frac{[s-\tau[1+\log(u)]]^2}{2\tau\log(u)}} \frac{ds}{\sqrt{2\pi\tau\log(u)}}\,du$$
$$\sim \tau^{3/2} \int_0^1 [-\log(u)]^{5/4} u^{\sqrt{\frac{\tau}{-8\pi\log(u)}}}\,du.$$

We thus conclude that while a power-law relationship persists between A_τ and τ, the scaling exponent is not related to the exponents of the power law of size (3/2) and duration (2) distribution through Sethna's crackling noise relationship, which would predict an exponent equal to 2. Importantly, we note that the exponent found here is quantitatively perfectly consistent with the exponent found in *in vitro* data [25] in the neural network model (Fig. 1) or surrogate Poisson system (Fig. 2).

IV. SPIKE PATTERN ENTROPY AND INFORMATION CAPACITY

We have thus proved that power-law distributions of avalanches do not necessarily reveal that the network is operating at criticality. However, a number of theories have proposed that operating at criticality was an optimal regime of information processing in the brain, perhaps selected by evolution as a useful trait for the nervous system [19,60,60–64]. The question that arises is thus whether these theories break down when power-law statistics no longer arise from the system operating at criticality but from a mean-field Boltzmann chaos regime.

In order to address this outstanding question, we came back to the methods used in order to demonstrate optimality of data processing capabilities at criticality. These theories rely on the computation of the information capacity of the network in different activity regimes evaluated, following Shannon's information theory, as the entropy of the patterns of spike fired. In detail, a spike pattern in a network of size N is an N-uplet $s \in \{0,1\}^N$, with $s_i = 1$ (respectively, $s_i = 0$) if neuron i has fired (respectively, not fired) in a specific time bin. If p denotes the probability of occurrence of spike patterns, then the entropy is given by:

$$\text{Entropy} = \sum_{s\in\{0,1\}^N} p(s)\log[p(s)].$$

In order to test whether our theory accounting for the emergence of power-law distributions in the absence of criticality challenges high information capacity of neuronal networks, we computed the information capacity of Brunel's model in different regimes (see Fig. 4). The numerical results show that this is not the case, and the information capacity is maximal in the SI regime where power-law statistics of avalanches were observed. However, we observe no difference

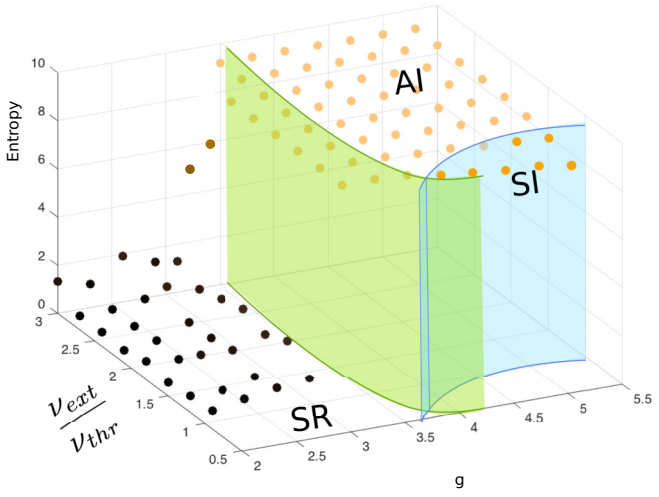

FIG. 4. Computation of the entropy (circles) of the network in the Brunel's model [27] for distinct values of the input intensity ν_{ext} and inhibition ratio g. The color code indicates the entropy amplitude. Parameters as in the original model [[27], Fig. 2(b)]. The blue surface represents the boundary between SI and AI regimes, and the green surface separates SR regimes from SI regimes. We observe a clear transition from low entropy (SR) to high entropy (SI+AI).

between entropy levels in the SI or AI states. Therefore, we conclude that the maximality of entropy is not necessarily related to the emergence of power-law statistics.

These observations can be well understood heuristically. Indeed, the entropy of spike patterns is a measure of the variability of possible spike patterns observed in the course of neuronal activity. The diagram of Fig. 4 is thus not surprising. Indeed, while the diversity of spike patterns is reduced in the highly synchronized regular regimes, it will be large in the irregular regimes, both synchronized asynchronous [65]. In other words, entropy is maximized within irregular regimes where more diverse patterns are fired, independently of the underlying mechanisms supporting the emergence of the irregular activity.

V. LOCAL FIELD POTENTIALS ARE AMBIGUOUS MEASURES OF CRITICALITY

We have thus shown that discarding the criticality assumption does not degrade the quantifications of network efficiency. This being said, we are facing an apparent contradiction. Indeed, our theory provides an account for the presence of critical statistics in networks in the SI regime but discards AI states as possibly having critically distributed avalanches. Evidence of critical statistics of avalanches *in vivo* in the awake brain have been reported but are more scarce and controversial. Unlike neuronal cultures, the activity in the awake brain does not display bursts separated by silences but is sustained. Using a macroscopic measurement of neuronal activity, the LFP, power laws could be shown from the distribution of peaked events [17]. The motivation to use negative LFP peaks to deduce information from the distribution of spike avalanches relied on the fact that the amplitude of these peaks correlated with firing activity [16,19].

However, this monotonic relationship between the number of spikes and the number of spikes does not imply that there should exist a relationship between the distribution of peak amplitude and avalanches. Moreover, it was shown that power laws naturally emerge from the random nature of the signal and the thresholding procedure used in this analysis, and, moreover, these power laws may not be statistically significant [21]. Indeed, no power-law scaling could be found from unit activity, which was better fit by double-exponential distributions [24]. These analyses rather suggest that the power-law statistics of LFP peaks do not reflect scale-invariant neural activity.

In an attempt to clarify this, we investigate here whether the distribution of LFP peaks can display power-law scaling in spiking networks or in their stochastic surrogates. To obtain a more biophysical model where LFP can be defined, we considered the current-based Vogels and Abbott model [66] which provides a biologically realistic model of spiking network displaying asynchronous irregular and synchronous regular states and in which synaptic currents are described by exponentially decaying functions with excitation and inhibition having distinct time constants (in place of Dirac impulses in the Brunel model (1) see Ref. [66] for details). Simulations of the model provide an instantaneous distribution of postsynaptic currents, from which we computed LFP signals.

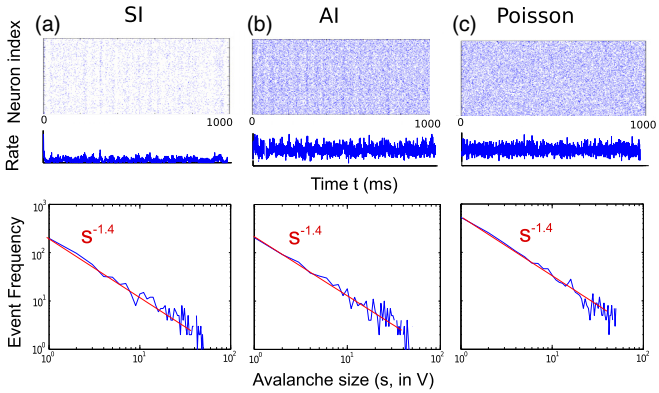

FIG. 5. Avalanche analysis defined from the macroscopic variable V_{LFP} of a network of integrate-and-fire neurons with exponential synapses. Networks displaying an SI (left) or AI (middle) state and a purely stochastic surrogate (right) show similar macroscopic power-law LFP peak statistics with the same exponent close to $-3/2$.

In detail, we have considered a spatially extended neural network of 5000 units randomly located on a two-dimensional square and satisfying the Vogels-Abbott model. We evaluated an LFP signal V_{LFP} from the postsynaptic currents according to Coulomb's law [67]:

$$V_{\mathrm{LFP}} = \frac{R_e}{4\pi} \sum_j \frac{I_j}{r_j},$$

where V_{LFP} is the electric potential at the electrode position, $R_e = 230\,\Omega$ cm is the extracellular resistivity of brain tissue, I_j are the synaptic currents of neuron j, and r_j is the distance between I_j and electrode position. Remarkably, applying to this more sophisticated model the same procedures as in the original paper [17], we found that the method cannot distinguish between structured or nonstructured activity: For a fixed firing rate and bin size, we have been comparing in Fig. 5 the LFP statistics of the avalanche duration in a network of neurons in the AI regime [Fig. 5(a)] or in the SI regime [Fig. 5(c)] that shows partial order of the firing and saw no difference. We also compared the statistics to those of independent Poisson processes with constant rate [Fig. 5(b)]: The three instances show power-law scaling of avalanche duration, with the same exponent, that seem to rather be related to the firing rate and bin size than to the form of the network activity. The scaling coefficient is, again, close to $3/2$ and varies with bin size. Clearly, in this case, the dynamics of LFP peaks cannot distinguish between critical and noncritical regimes.

VI. DISCUSSION

In this paper, we have evaluated how power-law statistics and universal scaling can arise in the absence of criticality. We first outline the novel contributions of the present manuscript, and then we discuss their significance.

The contributions of the present manuscript are as follows:

(i) We first investigated the avalanche statistics of spiking neural networks models (Sec. II). We showed that these networks display power-law statistics with the critical exponents

$-3/2$ and -2, as well as collapse of the shapes of avalanches. This observation is robust and valid for a wide region of parameters corresponding to synchronous irregular activity in such networks and thus away from any transition point (i.e., away from criticality).

(ii) This robust numerical observation led us to investigate theoretically how such statistics can emerge from the collective activity of spiking networks. One ubiquitous property of large neural networks models is that neurons behave as independent processes with the same statistics. This property, termed *Boltzmann's molecular chaos* regime in statistical physics, or *propagation of chaos* in mathematics, is universal in the dynamics of large-scale networks. We reviewed such properties in models, as well as recent experimental evidence supporting this decorrelation between the dynamics of cells.

(iii) We next tested the hypothesis that power laws may emerge from such large systems of weakly correlated units with similar statistics. We introduced and investigated numerically the dynamics of a surrogate network made of independent neurons sharing the same statistics (Sec. III C). Surprisingly, despite the simplicity of these systems, they display precisely the same power-law statistics of avalanche duration and size with the same exponents and shape collapse as fully connected networks.

(iv) This surrogate model is simple enough to derive in closed form the statistics of the duration and size of the avalanches. Using this analytic expression, we demonstrate that the "critical" exponents emerge naturally in large-scale systems (operating within the Boltzmann chaos regime), without the need to invoke criticality (Sec III D).

(v) Current literature indicate that criticality is an optimal information processing regime for the brain. We considered the same measures of information capability (entropy of spike trains) on our biologically plausible models and showed that, indeed, information is maximized in the SI regime where power laws emerge. However, we show that this is not exclusive of the SI regime but the same levels of entropy are found in AI regimes where no avalanche can be defined.

(vi) Finally, we also addressed the presence of power-law scalings observed in LFP recordings by simulating such signals emerging from more realistic neuronal network models with excitatory and inhibitory cells. Surprisingly, we observed that power laws with the same exponents as observed in experiments are found in all regimes tested. These exponents persisted when neurons were replaced by independent Poisson processes. This clearly indicates that power-law scalings in LFPs do not constitute any proof of criticality in the underlying system.

All together, these numerical and theoretical findings provide a new interpretation for the emergence of power-law statistics in large-scale systems, independent of the notion of criticality. We propose to explain the emergence of such scaling based on Boltzmann molecular chaos regime, known to govern the dynamics of most large-scale interacting systems [27,36,40]. In other words, power-law and universal scaling functions can be due to a mean-field effect in systems made of a large number of interacting units. Of course, this theory does not hypothesize that the elements considered (here, neurons) are disconnected in reality. To the contrary, the fact that the critical exponents still resist the removal of interconnections shows that such exponents do not need criticality to be explained.

The main mechanism explored here, Boltzmann's molecular chaos, is a universal feature of many statistical systems. The very particular structure of different particles activity it induces, namely statistical independence of the particles behavior together with a correlation in the law, may induce as we have observed, the same type of power laws as in critical systems, with universal coefficients that are consistent with those found in critical systems. In agreement with this theory, we have seen that the same statistics are reproduced by a sparsely connected network and a surrogate stochastic process where the periods of firing and silences are themselves generated by another stochastic process. This interpretation suggests that similar scaling relationships shall arise in more realistic neural network models with fixed connectivity patterns, in particular including axonal propagation delays (constant delays are already present in Brunel model), dendritic structure, spike frequency adaptation, and noninstantaneous synaptic transmission. Indeed, most of these elements will make the intrinsic dynamics of each cell more complex, but we do not expect that this complexity could affect the fact that these systems operate within the Boltzmann molecular chaos regime. Notwithstanding, models including synaptic plasticity, which is the process by which the brain acquires skills and stores memories, may not belong to the class of systems described in this paper. Indeed, in such systems, the connectivity patterns vary depending on the pairwise correlations of cells activity, and this relationship may compete with the establishment of Boltzmann's molecular chaos regime. While this may not occur in the adult brain where plasticity is much slower than neuronal activity, distinct phenomena not described by our model may occur occur during the critical periods of brain development, when plasticity occurs at a faster time scale. Further experimental and theoretical investigations are necessary to characterize avalanche distributions in these systems, as well as to compute correlation levels to test if the decorrelation characteristic of Boltzmann's molecular chaos occurs.

Interestingly, a network operating in Boltzmann's molecular chaos regime can be interpreted as a high-dimensional system with hidden variables, as studied recently in Refs. [68,69]. In these contributions, the authors investigate the rank distribution of high-dimensional data with hidden latent variable and show that such systems display Zipf law scaling (power laws with slope -1 in the rank distribution) that generically arise from entropy consideration and use the elegant identity between entropy and energy shown in Ref. [70]. While these developments do not generalize here, Boltzmann molecular chaos provides a natural explanation for the emergence of weakly correlated units with similar probability laws: In the neural network system case, the common rate could be seen as a latent variable, and both independence and irregularity build up only from the interactions between cells. As a result of this theory, revealing apparent power-law scaling with exponents of $-3/2$ and 2, as well as shape collapse, may be entirely explained statistically; in particular, these criteria constitute no proof of criticality and experimental studies solely relying on them should be re-evaluated.

This statement is even more true when it comes to macroscopic measurements such as the LFP: Both SI and AI regimes,

as well as stochastic surrogates, display power-law statistics in the distribution of LFP peaks. This shows that systems of weakly correlated units, or their stochastic surrogates, can generate power-law statistics when considered macroscopically. Here again, the power-law statistics tells nothing about the critical or noncritical nature of the underlying system. This potentially reconciles contradictory observations that macroscopic brain variables display power-law scaling [17], while no sign of such power-law scaling was found in the units [24,71]. More generally, these results also put caution on the interpretation of power-law relations found in nature.

A question that naturally emerges is how to distinguish power laws due to criticality from those due to Boltzmann's molecular chaos regime. We used the previous observation [26] that a prominent characteristic of criticality beyond the presence of power-law scalings is the particular relationship one finds between the exponents. We found here that the power-law scalings emerging in the absence of criticality did not satisfy this relationship. We propose to use that criterion as a possible way to distinguish between power-law scaling due to criticality or due to Boltzmann's molecular chaos.

In conclusion, we have shown here that stochastic models can replicate many of the experimental observations about "critical" exponents, which demonstrates that not only is power-law scaling not enough to prove criticality but also we need new and better methods to investigate this in experimental systems. The fact that such exponents are seen for networks and for stochastic systems shows that they apply to a large class of natural systems and may be more universal than previously thought. As Georges Miller noticed in his seminal paper [8] examining random text typed by virtual monkeys, the texts produced may not be interesting but have *some of the statistical properties considered interesting when humans, rather than monkeys, hit the keys.* Similarly, the present results show systems that can emulate the power-law scaling seen in brain activity but with no criticality involved. We thus cannot conclude on whether the brain operates at criticality or not, but we need more elaborate methods to resolve this point.

ACKNOWLEDGMENTS

A.D. was supported by the ICODE Excellence network and grants from the European Community (BrainScales FP7-269921 and Human Brain Project FP7-604102 and H2020-720270). We warmly thank Quan Shi and Roberto Zuñiga Valladares for preliminary work and analyzes. We thank anonymous referees for their suggestions of analyses and references.

APPENDIX A: POWER-LAW STATISTICS AND MAXIMUM LIKELIHOOD FITS FOR STATIONARY DATA

We review here the methods used to fit the power-law distributions that closely follow the methodology exposed in Ref. [30]. This methodology applies to stationary data. Taking the logarithm of the probability density of a power-law random variable, we obtain $\log[p(x)] = -\alpha \log(x) + \log(a)$. The histogram of the power law therefore presents an affine relation in a log-log plot. For this reason, power laws in empirical data are often studied by plotting the logarithm of the histogram as a function of the logarithm of the values of the random variable and doing a linear regression to fit an affine line to through the data points (usually using a least-squares algorithm). This method dates back to Pareto in the 19th century (see e.g., Ref. [72]). The evaluated point $\hat{x}_{\min}$ corresponding to the point where the data start having a power-law distribution is mostly evaluated visually, but this method is very sensitive to noise (see, e.g., Ref. [73] and references herein). The maximum likelihood estimator of the exponent parameter α corresponding to n data points $x_i \geqslant x_{\min}$ is

$$\hat{\alpha} = 1 + n\left(\sum_{i=1}^{n} \log \frac{x_i}{x_{\min}}\right)^{-1}.$$

The log-likelihood of the data for the estimated parameter value is as follows:

$$L(\hat{\alpha}|X) = n \log\left(\frac{\hat{\alpha}-1}{x_{\min}}\right) - \hat{\alpha}\sum_{i=1}^{n} \log\left(\frac{x_i}{x_{\min}}\right).$$

The parameter $\hat{x}_{\min}$ is evaluated then by minimizing the Kolmogorov-Smirnov distance:

$$KS = \max_{x \geqslant x_{\min}} |S(x) - \hat{P}(x)|,$$

where $S(x)$ is the cumulative distribution function (CDF) of the data and $\hat{P}(x)$ is the CDF of the theoretical distribution being fitted for the parameter that best fits the data for $x \geqslant x_{\min}$), as proposed by Clauset and colleagues in Ref. [74]. In order to quantify the accuracy of the fit, we use a standard goodness-of-fit test which generates a p-value. This quantity characterizes the likelihood of obtaining a fit as good or better than that observed if the hypothesized distribution is correct. This method involves sampling the fitted distribution to generate artificial data sets of size n and then calculating the Kolmogorov-Smirnov distance between each data set and the fitted distribution, producing the distribution of Kolmogorov-Smirnov distances expected if the fitted distribution is the true distribution of the data. A p-value is then calculated as the proportion of artificial data showing a poorer fit than fitting the observed data set. When this value is close to 1, the data set can be considered to be drawn from the fitted distribution, and, if not, the hypothesis might be rejected. The smallest p-values often considered to validate the statistical test are taken between 0.1 and 0.01. These values are computed following the method described in Ref. [30], which in particular involves generating artificial samples through a Monte Carlo procedure.

These methods, very efficient for stationary data, fail to evaluate the tails of nonstationary data as is the case for neuronal data. A weighted Kolmogorov-Smirnov test with a refined goodness-of-fit estimate is valid up to extreme tails [75].

APPENDIX B: SUBSAMPLING EFFECTS

Of course, any analysis of finite sequences of data is subject to subsampling effects. While these may be neglected for light-tailed data, they become prominent when it comes to assessing possible slow decay of the tails of a statistical sample distribution. These effects were discussed in detail in a number

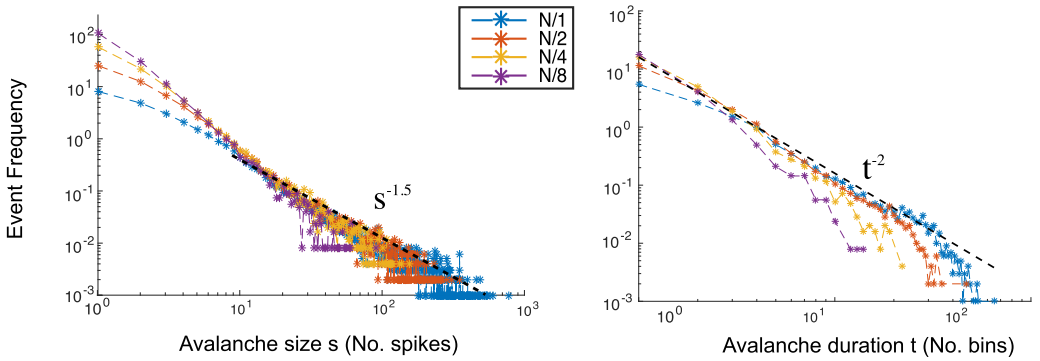

FIG. 6. Subsampling effects. Statistics for a randomly extracted subset of neurons of size $n = 125,250,500$, among 1000 neurons whose dynamics is described by Brunel's model. Theoretical power laws with critical exponents are displayed with black dashed lines.

of contributions. In the context of neuronal avalanches, these effects were characterized in Ref. [76], and the results show indeed a modification of the slope with subsampling, together with exponential cutoffs pushed to larger sizes as sampling becomes finer.

We have confirmed these results in our own data. In Fig. 6, we have computed the distribution of avalanche size and duration when considering only a fraction of the neurons for the statistics. In detail, we have simulated the Brunel model [27] with $N = 1000$. This yields a raster plot, from which we have extracted a randomly chosen subset of n neurons, with $n = N/k$ for $k \in \{2,4,8\}$. We indeed observed that an exponential cutoff is shifted towards larger sizes and slopes increase with the subsampling ratio k.

APPENDIX C: BRUNEL'S MODEL

In our simulations, we have used the neuronal network model introduced by Brunel [27] and have referred to the different dynamical regimes of this system. We review here the model, provide all parameters used in our simulations, and show that the conclusions drawn in one example of the SI state are valid for all parameters tested within this regime. The model describes the dynamics of N integrate-and-fire neurons, 80% of which are excitatory and the others inhibitory. In the model, it is assumed that each neuron receives $C = \varepsilon N$ randomly chosen connections, that are assumed to uniformly arise from the excitatory and the inhibitory population, thus 80% of the incoming connections to any cell come from the excitatory population. The network is assumed to be sparsely connected, thus $\varepsilon \ll 1$. The depolarization v^i of neuron i at the soma satisfies the equation:

$$\tau \frac{dv^i}{dt} = -v^i + RI_i(t),$$

where $I_i(t)$ is the total current reaching the soma at time t. These currents arrive from the synapses made with other cells within the network, as well as from connections to neurons outside the network. It is assumed that each neuron receives C_{ext} connections to and from excitatory neurons outside the network and that these synapses are activated by independent Poisson processes with rate ν_{ext}. The current receives by neuron i is thus the sum:

$$RI_i(t) = \tau \sum_{j=1}^{C+C_{\text{ext}}} J_{ij} \sum_k \delta\left(t - t_j^k - D\right),$$

where the sum is taken over all synapses, J_{ij} are the synaptic efficacies, t_j^k are the spike times at synapse j of neuron i, and D is the typical transmission delay, considered homogeneous at all synapses for simplicity. In order to simplify further the model, it is assumed that $J_{ij} = J > 0$ for all excitatory synapses, and $J_{ij} = -gJ < 0$ for inhibitory synapses. The parameter g is relevant in that it controls the balance between excitation and inhibition: If $g < 4$, then the network is dominated by excitation, and otherwise it is dominated by inhibition. The neuron i fires an action potential when v^i reaches a fixed threshold θ, and the depolarization of neuron i is instantaneously reset to a fixed value V_r where it remains fixed during a refractory period τ_{rp} (during this period, the neuron is insensitive to any stimulation). An important parameter is the ratio between the rate of external input ν_{ext} and the quantity denoted ν_{thresh} corresponding to the minimal frequency that can drive one neuron, disconnected from the network, to fire an action potential: $\nu_{\text{thresh}} = \frac{\theta}{0.8J\tau}$ (the coefficient 0.8 in that formula corresponds to the fraction of excitatory neurons).

In this model, the parameters that are kept free are the balance between excitation and inhibition g and the external firing rate ν_{ext}. All other parameters are chosen as in Table I using a mean-field analysis together with a diffusion approximation, the authors find that all neurons are independent point process driven by a common rate $\nu(t)$ given by a self-consistent equation. Heuristically, during the time interval $[t, t + dt]$, the probability for any given to spike is given by $\nu(t)\,dt$, and the realization of this random variable are independent in the different neurons. When the rate $\nu(t)$ depends on time, neurons thus show a level of synchrony, and when $\nu(t)$ is constant, the regime is called asynchronous, in the parlance of Ref. [27]. In that paper, an analysis of the self-consistent rate equation in

TABLE I. Parameters used in all simulations of Brunel's model, as in Ref. [27].

ε	D	J	τ_{rp}	θ	V_r
0.1	1.8 ms	0.2 mV	2 ms	20 mV	10 mV

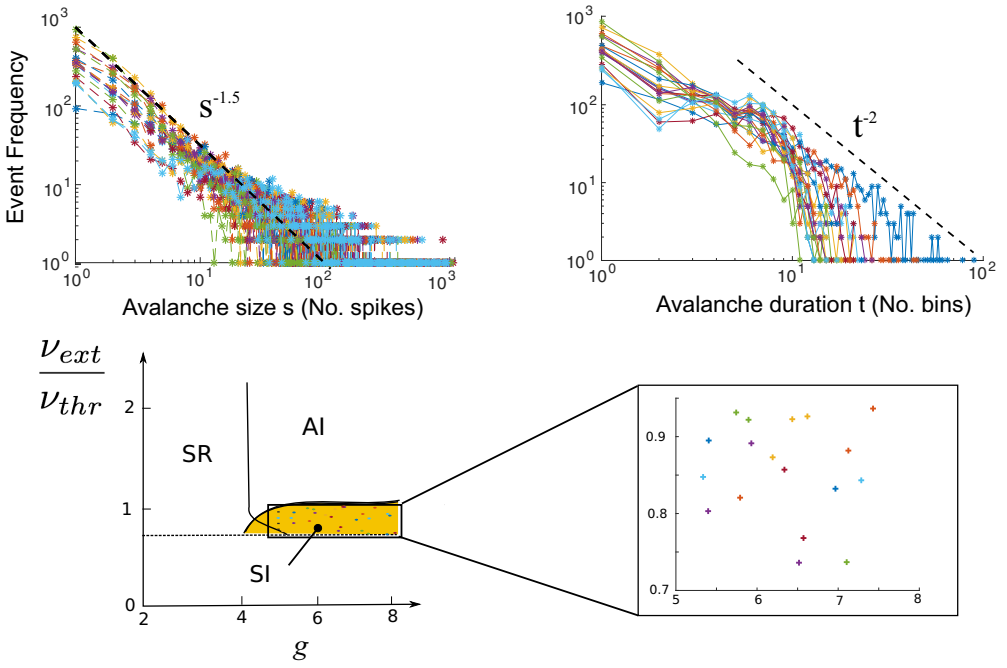

FIG. 7. Avalanche statistics for the Brunel model with randomly chosen parameters within the SI regime.

the mean-field limit led to the identification of several regimes that are depicted in Fig. 7:

(i) The AI state in which $\nu(t)$ converges towards a strictly positive constant value, which occurs when the excitatory external inputs are sufficiently large ($\nu_{\text{ext}} > \nu_{\text{thresh}}$) and when inhibition dominates excitation.

(ii) The SR regime corresponds to a state in which $\nu(t)$ is a periodic function of time. This regimes arises in the excitation dominated regime, and the oscillation frequency is controlled essentially by the transmission delay D and the refractory period τ_{rp} (approximately varying as τ_{rp}/D). The transition thus occurs close from the line $g = 4$.

(iii) The SI regime occurs essentially in the inhibition-dominated regime when the input are not sufficient to drive the network to a sustained firing state, i.e., when $\nu_{\text{ext}} < \nu_{\text{thresh}}$.

We have reproduced in Fig. 7 the bifurcation diagram [[27], Fig. 2(b)] with the bifurcation lines among the AI, SI, and SR states. Within the SI state, we have been randomly drawing 30 parameter points and analyzed the avalanches arising for these parameters. We have found that all regimes show a very clear power-law distribution of avalanche size and duration with exponents consistent with the exponents -1.5 and -2 predicted by the theory.

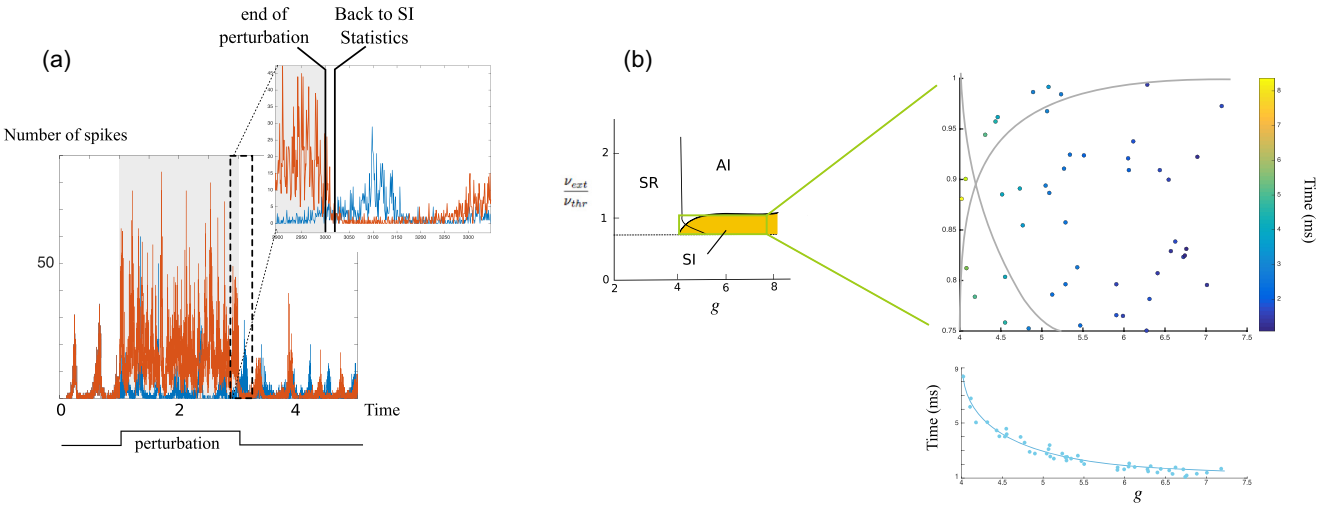

FIG. 8. Relaxation time of the Brunel model in the SI regime. (a) Typical trajectory (blue) perturbed by a constant input (red) into a SI regime returns to the SI state after a few milliseconds. This is true over the whole SI domain (b): Relaxation times are on the order of a few milliseconds and increase sharply close from the transition.

APPENDIX D: NO SLOWING DOWN WITHIN THE SI REGIME

In addition to the fact that the SI regime is away from any transition between the different network regimes, we confirmed that the system did not show the typical properties of critical states. A number of criteria were proposed in the Ising model to be characteristic of the critical regime. These include the divergence of the correlation length and of the heat capacity or magnetic susceptibility, which are all related to long-range correlations between spins. Here, the absence of the order parameter and spatial dimension prevents us from using similar criteria to investigate the presence of critical dynamics. However, a criterion independent of the definition of an analogous of order parameter or magnetic susceptibility is the *critical slowing down* occurring at phase transitions for dynamical systems. This criterion states that the relaxation time of the system, namely the time it takes for the system to return to its stationary regime after a perturbation, diverges at criticality.

In the present case, computing relaxation times is a challenge since the system is not at an equilibrium but within a chaotic regime, thus all perturbations produce massive changes in the dynamics of the system. Following the methodology developed in Refs. [77,78], we designed a numerical criterion to evaluate relaxation time to the SI regime. That regime is essentially defined by the alternation of periods of collective activity followed by silences. We have thus perturbed the system by adding a constant input within a short time window [see Fig. 8(a)], which has the effect of switching the system into an asynchronous irregular regime where the firing is uninterrupted. As the perturbation stops, the system quickly returns to an SI regime with alternations of silences and collective bursts. An upper bound of the relaxation time can thus be defined as the first time, after the perturbation has stopped, at which the system is completely silent. We have made extensive simulations within the SI regime to compute the relaxation time and obtained that the system returns to SI statistics after a few milliseconds after stimulation (on the order of 2 ms). This time increases very fast close to the SI-AI transition as expected from the theory, but within the SI regime, the system did not show any indication of critical slowing down.

APPENDIX E: DIVERSE REGIMES OF INDEPENDENT PROCESSES

We have confirmed that the statistics of independent Poisson processes with fluctuating instantaneous firing rates produce avalanches with power-law distributions of avalanche size and durations, consistent with our theory. To this purpose, we have performed a similar analysis as in Fig. 2, replacing Ornstein-Uhlenbeck firing rates with the positive part of a Brownian motion reflected at ± 1. This choice was motivated by two constraints: The positive part was taken in order to consider only positive firing rates for consistency, and the reflection at ± 1 was forced in order to prevent us from having too-long excursions of the Brownian motion, so we can indeed assess that the heavy tails of the avalanche distributions are rather due to the statistical structure of the firing rather than to very long excursions of the Brownian motion. The results of the simulations are provided in Fig. 9. As in the case of the positive part of the Ornstein-Uhlenbeck process, we find very clear power-law distributions of avalanche size and durations, with slopes consistent with our theory, and a very clear collapse of the avalanche shapes.

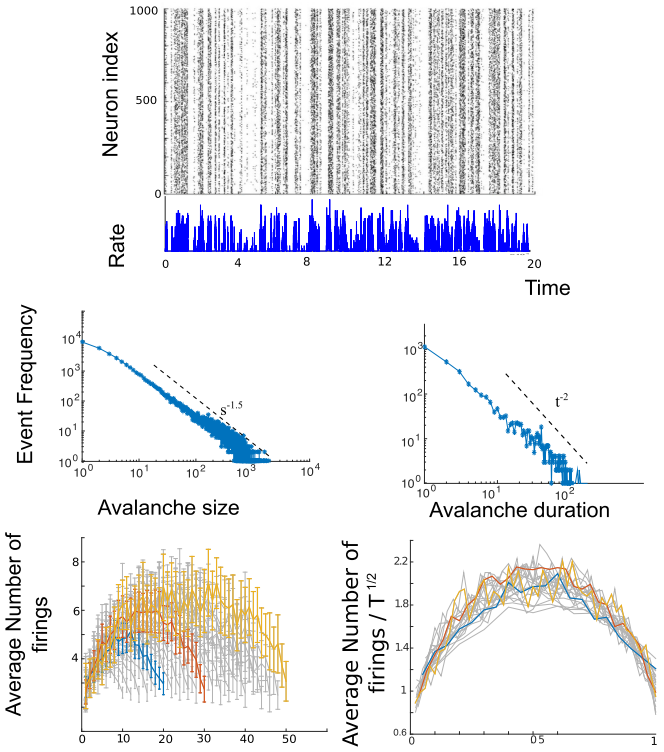

FIG. 9. Avalanche statistics and shape collapses for independent Poisson processes with rates given by a reflected Brownian motion.

We add that, beyond the collapse of the avalanche trajectories, the shapes on these avalanche collapses may convey important information, as noted and investigated in the context of one-dimensional random walks [22,23]. We observe indeed that the shape of the network-generated avalanches are not similar to the shapes obtained in the Brownian or Ornstein-Uhlenbeck cases and may similarly contain information that goes beyond pure shape collapse reported in neural data [25].

[1] P. Bak, *How Nature Works* (Oxford University Press, Oxford, 1997).
[2] H. J. Jensen, *Self-Organized Criticality: Emergent Complex Behavior in Physical and Biological Systems*, Vol. 10 (Cambridge University Press, Cambridge, 1998).
[3] M. E. Newman, Contemp. Phys. **46**, 323 (2005).
[4] M. Kardar, *Statistical Physics of Fields* (Cambridge University Press, Cambridge, 2007).
[5] P. Bak, C. Tang, and K. Wiesenfeld, Phys. Rev. Lett. **59**, 381 (1987).
[6] M. P. Stumpf, M. A. Porter *et al.*, Science **335**, 665 (2012).

[7] D. Avnir, O. Biham, D. Lidar, and O. Malcai, Science **279**, 39 (1998).
[8] G. A. Miller, Am. J. Psychol. **70**, 311 (1957).
[9] W. Li, IEEE Trans. Inf. Theory **38**, 1842 (1992).
[10] J. Bouchaud, in *Lévy Flights and Related Topics in Physics* (Springer, Berlin, 1995), pp. 237–250.
[11] N. Jan, L. Moseley, T. Ray, and D. Stauffer, Adv. Complex Syst. **2**, 137 (1999).
[12] H. Takayasu, M. Takayasu, A. Provata, and G. Huber, J. Stat. Phys. **65**, 725 (1991).
[13] H. Takayasu, I. Nishikawa, and H. Tasaki, Phys. Rev. A **37**, 3110 (1988).
[14] H. Takayasu, Phys. Rev. Lett. **63**, 2563 (1989).
[15] M. Benayoun, J. D. Cowan, W. van Drongelen, and E. Wallace, PLoS Comput. Biol. **6**, e1000846 (2010).
[16] Y. Dan, J. J. Atick, and R. C. Reid, J. Neurosci. **16**, 3351 (1996).
[17] T. Petermann, T. C. Thiagarajan, M. A. Lebedev, M. A. Nicolelis, D. R. Chialvo, and D. Plenz, Proc. Natl. Acad. Sci. U.S.A. **106**, 15921 (2009).
[18] G. Hahn, T. Petermann, M. N. Havenith, S. Yu, W. Singer, D. Plenz, and D. Nikolić, J. Neurophysiol. **104**, 3312 (2010).
[19] W. L. Shew and D. Plenz, Neuroscientist **19**, 88 (2013).
[20] D. R. Chialvo, Nat. Phys. **2**, 301 (2006).
[21] J. Touboul and A. Destexhe, PloS ONE **5**, e8982 (2010).
[22] F. Colaiori, A. Baldassarri, and C. Castellano, Phys. Rev. E **69**, 041105 (2004).
[23] A. Baldassarri, F. Colaiori, and C. Castellano, Phys. Rev. Lett. **90**, 060601 (2003).
[24] N. Dehghani, N. G. Hatsopoulos, Z. D. Haga, R. A. Parker, B. Greger, E. Halgren, S. S. Cash, and A. Destexhe, Front. Physiol. **3**, 302 (2012).
[25] N. Friedman, S. Ito, B. A. W. Brinkman, M. Shimono, R. E. Lee DeVille, K. A. Dahmen, J. M. Beggs, and T. C. Butler, Phys. Rev. Lett. **108**, 208102 (2012).
[26] J. P. Sethna, K. A. Dahmen, and C. R. Myers, Nature **410**, 242 (2001).
[27] N. Brunel, J. Comput. Neurosci. **8**, 183 (2000).
[28] We used the algorithm freely available on ModelDB.
[29] Subsampling of the network may lead to find periods of quiescence, whose statistics will depend on the network size. However, these are not robust statistical quantities to define a critical regime.
[30] A. Clauset, C. R. Shalizi, and M. E. Newman, SIAM Rev. **51**, 661 (2009).
[31] The Kolmogorov-Smirnov statistical tests are not affected by events of very small frequency.
[32] L. Boltzmann, *Lectures on Gas Theory* (University of California Press, Berkeley, Los Angeles, California, 1964).
[33] A. Renart, N. Brunel, and X.-J. Wang, *Computational Neuroscience: A Comprehensive Approach*, edited by J. Feng (Chapman and Hall CRC Press, Boca Raton, 2004), pp. 431–490.
[34] H. Sompolinsky, A. Crisanti, and H. J. Sommers, Phys. Rev. Lett. **61**, 259 (1988).
[35] S. Ostojic, Nat. Neurosci. **17**, 594 (2014).
[36] A. Sznitman, Ecole d'Eté de Probabilités de Saint-Flour XIX, 165 (1989).
[37] P. Robert and J. D. Touboul, J. Stat. Phys. **165**, 545 (2016).
[38] J. Touboul, G. Hermann, and O. Faugeras, SIAM J. Appl. Dynam. Syst. **11**, 49 (2012).
[39] S. Mischler, C. Quiñinao, and J. Touboul, Commun. Math. Phys. **342**, 1001 (2016).
[40] J. Touboul, Ann. Appl. Probab. **24**, 1298 (2014).
[41] J. Touboul, J. Stat. Phys. **156**, 546 (2014).
[42] A.-S. Sznitman, J. Funct. Anal. **56**, 311 (1984).
[43] T. Cabana and J. Touboul, J. Stat. Phys. **153**, 211 (2013).
[44] D. L. Ruderman, Netw. Comput. Neur. Syst. **5**, 517 (1994).
[45] D. L. Ruderman and W. Bialek, Phys. Rev. Lett. **73**, 814 (1994).
[46] D. W. Dong and J. J. Atick, Netw. Comput. Neur. Syst. **6**, 159 (1995).
[47] Y. Dan, J. J. Atick, and R. C. Reid, J. Neurosci. **16**, 3351 (1996).
[48] F. Attneave, Psychol. Rev. **61**, 183 (1954).
[49] H. B. Barlow, in *Sensory Communication*, edited by W. A. Rosenblith (MIT Press, Cambridge, MA, 1961), pp. 217–234.
[50] S. Laughlin, Z. Naturforsch. **36**, 910 (1981).
[51] E. P. Simoncelli and B. A. Olshausen, Annu. Rev. Neurosci. **24**, 1193 (2001).
[52] A. Dimitrov and J. D. Cowan, Neural Comput. **10**, 1779 (1998).
[53] A. Peyrache, N. Dehghani, E. N. Eskandar, J. R. Madsen, W. S. Anderson, J. A. Donoghue, L. R. Hochberg, E. Halgren, S. S. Cash, and A. Destexhe, Proc. Natl. Acad. Sci. U.S.A. **109**, 1731 (2012).
[54] A. Ecker, P. Berens, G. Keliris, M. Bethge, N. Logothetis, and A. Tolias, Science **327**, 584 (2010).
[55] A. Renart, J. De la Rocha, P. Bartho, L. Hollender, N. Parga, A. Reyes, and K. Harris, Science **327**, 587 (2010).
[56] X.-J. Wang, Y. Liu, M. V. Sanchez-Vives, and D. A. McCormick, J. Neurophysiol. **89**, 3279 (2003).
[57] M. T. Wiechert, B. Judkewitz, H. Riecke, and R. W. Friedrich, Nat. Neurosci. **13**, 1003 (2010).
[58] L. Alili, P. Patie, and J. L. Pedersen, Stochastic Models **21**, 967 (2005).
[59] W. Feller, *An Introduction to Probability Theory and Its Applications*, Vol. 2 (John Wiley & Sons, New York, 2008).
[60] W. L. Shew, H. Yang, S. Yu, R. Roy, and D. Plenz, J. Neurosci. **31**, 55 (2011).
[61] J. Hesse and T. Gross, Front. Syst. Neurosci. **8**, 166 (2014).
[62] W. L. Shew, H. Yang, T. Petermann, R. Roy, and D. Plenz, J. Neurosci. **29**, 15595 (2009).
[63] J. M. Beggs and N. Timme, Front. Physiol. **3**, 163 (2012).
[64] J. Beggs, Philos. Trans. Roy. Soc. Lond. A **366**, 329 (2008).
[65] In the models based on branching processes with parameter p, it is clear that the maximal diversity arises at criticality, where the entropy is larger than in the subcritical regime (only patterns with a small number of spikes) or in the supercritical regime $p > 1$ (patterns with a large number of spikes).
[66] T. P. Vogels and L. F. Abbott, J. Neurosci. **25**, 10786 (2005).
[67] P. L. Nunez and R. Srinivasan, *Electric Fields of the Brain: The Neurophysics of EEG* (Oxford University Press, Oxford, 2006).
[68] L. Aitchison, N. Corradi, and P. E. Latham, PLOS Comput. Biol. **12**, e1005110 (2016).

[69] D. J. Schwab, I. Nemenman, and P. Mehta, Phys. Rev. Lett. **113**, 068102 (2014).
[70] T. Mora and W. Bialek, J. Stat. Phys. **144**, 268 (2011).
[71] C. Bedard, H. Kroger, and A. Destexhe, Phys. Rev. Lett. **97**, 118102 (2006).
[72] B. Arnold, *Pareto Distributions* (International Co-operative, Fairland, Md, 1983).
[73] S. A. Stoev, G. Michailidis, and M. S. Taqqu, IEEE Trans. Inf. Theor. **57**, 1615 (2011).
[74] A. Clauset, M. Young, and K. Gleditsch, J. Conflict Resol. **51** (2007), doi:10.1177/0022002706296157.
[75] R. Chicheportiche and J.-P. Bouchaud, Phys. Rev. E **86**, 041115 (2012).
[76] V. Priesemann, M. H. Munk, and M. Wibral, BMC Neurosci. **10**, 40 (2009).
[77] R. Engelken, F. Farkhooi, D. Hansel, C. van Vreeswijk, and F. Wolf, F1000Research **5** (2016).
[78] Z. Girones and A. Destexhe, arXiv:1611.09089 (2016).